

TOWARDS THE 'IN VIVO' COMPUTATIONAL MULTI-SCALE HEMODYNAMICS FROM ENDOTHELIAL CELL TO LARGE ARTERY

H. Liu^{1,2}, H. Iwase², N. Matsunaga², Y. He², K. Yokoi² and R. Himeno²

¹Department of Electronics and Mechanical Engineering, Faculty of Engineering
Chiba University, Chiba, Japan

²Computer and Information Division, RIKEN, Saitama, Japan

Abstract. A prototype, multi-scale, computational hemodynamic model is presented. Applications to aortic arch, carotid artery, renal artery and so forth, has demonstrated its feasibility in medical applications of the computation-based diagnosis and surgery; and with this novel multi-scale computational method in hemodynamics the noninvasive simulation of cardiovascular blood flow would become possible. We have recently developed a multi-scale, computational method that is able to predict blood flow and pressure in the systematic arteries at any position along the vessels, to compute local flow patterns as well as wall shear stresses at any point in any vessel or organ, and further to predict the behavior of the endothelial cells subjected to the local wall shear stress. A one-dimensional model is established on a basis of the axisymmetric Navier-Stokes equations for flow and pressure propagation in compliant and tapering vessels. The three-dimensional model is utilized for specific vessel or organ, which is an in-house solver for the full Navier-Stokes equations and is embedded into the one-dimensional network model for the systematic arteries.

1. Introduction

Blood dynamics in cardiovascular system involve length scales in vastly different ranges, entailing dimensions from cell surface receptors on the *nm* order up to large arteries with *cm* length. Hemodynamics is of multi-scale physical phenomena but conventional theories are mostly established at the individual levels of scale. Multi-scale method can break the whole work into individual but interactive domains, making the approach practical and promising for tackling the vast scale present in hemodynamics.

An overall view of the hemodynamics in circulation system is schematically illustrated in Fig. 1. At the level of global circulation system with a meter-size scale, hemodynamics is characterized by the flow and pressure propagation in a multi-branching, network with compliant and tapering vessels; and the feature can be predicted efficiently using the zero or one-dimensional model based on either the lumped parameter model or the axisymmetric Navier-Stokes equations. The macro-hemodynamics at the level of *cm*-scale that usually points to some specific large vessel or organ often show a rich variety of vortical flows and separation as a result of the dynamic pulsation of the blood flow, and the richness & complexity of the geometry of vessels or organs. This blood flow characteristics can help us to understand the detailed information of the complex flow fields with applications to wall shear stress (WSS), a major factor in the onset, the development, and the outcome of the arteriosclerosis. Here, full Navier-Stokes equations need to be resolved under appropriate boundary conditions associated with flow and pressure so as to explain the feature of the time-varying WSS distribution in space and in time. Further scaling down to the level of *mm*-scale, we have a view of microcirculation in the capillaries where the mass transport of blood cells, oxygen and ADP, etc functions in nutrient and waste transport; and the meso-hemodynamics treats the blood as two-phase or multi-phase fluid, i.e., a mixture of plasma (water, proteins, enzymes, etc.) and blood cells rather than the Newtonian fluid. At the cell level of μm -scale, the micro-hemodynamics often points to the cell biomechanics that deals with the deformation and remodeling of the arterial endothelial cells under wall shear stress stimulation as well as the mass transport across the endothelium, which are of fundamental importance

because it may provide important insight into understanding of arterial disease, e.g., atherogenesis. At the single molecular level of *nm*-scale, the nano-hemodynamics deals with the mechanics of a single molecular, e.g., the platelet and the gene may play a key role, but most remain unknown. Therefore, to stack up the individual hemodynamics in forming a “whole” hemodynamics in cardiovascular system may deepen our understanding of interrelationship among the scales and hence provide a novel global view of the hemodynamics; and the computational biomechanics is capable to make the approach practical and promising for this huge milestone.

As the first step, with consideration of medical application in computation-aided diagnosis and surgery, we believe that a computational, multi-scale, macro-hemodynamic method that combines the one-dimensional modeling for global flow and pressure propagation and the three-dimensional modeling for local wall shear stress under normal physiological and abnormal conditions may be feasible by taking into account of the interrelated interactions at the levels. We have developed such a method that is able to predict blood flow and pressure in the systematic arteries at any position along the vessels and to compute local flow patterns as well as wall shear stresses at any point in any vessel or organ. A one-dimensional model is established on a basis of the axisymmetric Navier-Stokes equations for flow and pressure propagation in compliant and tapering vessels. The three-dimensional model is utilized for specific vessel or organ, which is an in-house solver for the full Navier-Stokes equations and is embedded into the one-dimensional network model for the systematic arteries. We present some preliminary results for a comprehensive study on blood flow in a human aortic arch and demonstrate that the multi-scale computation in hemodynamics provides a noninvasive simulation-based tool for cardiovascular blood flow.

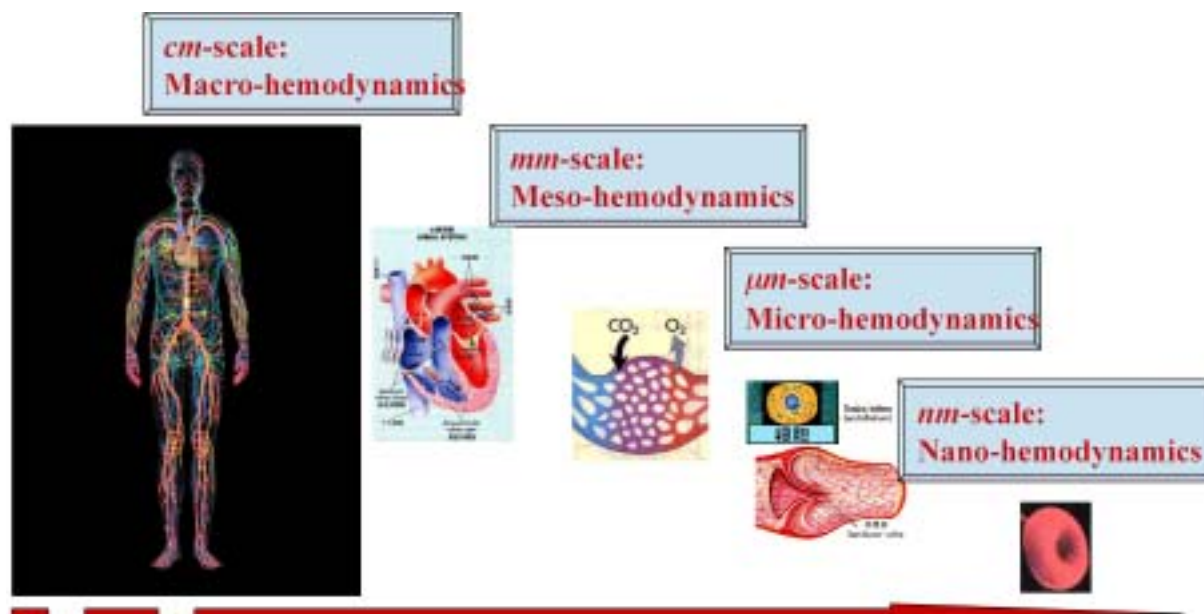


Fig. 1 Schematic diagram of multi-scale computation in hemodynamics

2. Multi-scale computation in hemodynamics

2.1 One-dimensional modeling of pulsatile wave in systematic arteries

An axisymmetric one-dimensional model of blood vessels

Following Olufsen et al. we constructed a systematic arterial tree as illustrated in Fig. 2, which is modeled as a binary tree where the geometry of the vessels may be determined from the measured medical images, e.g., MRI or based on general statistical relationships that are estimated from literature data. A typical vessel in this tree is modeled as an axisymmetric compliant cylinder; and hence computation of flow rate and pressure in the compliant vessel requires an equation of mass or volume, an equation of momentum, and an equation of state, such that,

$$\frac{\partial A}{\partial t} + \frac{\partial q}{\partial x} = 0, \tag{1}$$

$$\frac{\partial q}{\partial t} + \frac{\partial}{\partial x} \left(\frac{q^2}{A} + B \right) = -\frac{2\pi v q R}{\delta A} + C, \tag{2}$$

$$p(x,t) - p_0 = \frac{4}{3} \frac{Eh}{r_0} \left(1 - \sqrt{\frac{A_0}{A}} \right), \tag{3}$$

where

$$B = \frac{4}{3} \frac{Eh}{r_0} \frac{\sqrt{A_0 A}}{\rho}, C = \frac{\partial B}{\partial x} - \frac{A}{\rho} \frac{\partial p}{\partial x},$$

$$\frac{Eh}{r_0} = k_1 \exp(k_2 r_0) + k_3$$

Here $q(x,t)$ denotes flow rate; $p(x,t)$ is pressure that does not vary over the cross-section; $A(x,t)$ is area of the cross-section that corresponds to the radius $R(x,t)$; ρ is density; v is viscosity; and r_0 is the radius when the pressure equals to the diastole pressure $p(x,t)=p_0$. Note that δ represents the boundary layer thickness for the large arteries, approximately 0.1cm. The vessel is assumed to taper exponentially, i.e., the equilibrium radius is $r_0(x)=r_{top} \exp(\log(r_{bot}/r_{top})x/L)$ when $p(x,t)=p_0$. The r_{top} and r_{bot} denote the inlet (top) and outlet (bottom) radii of the vessel. Note that, in order to keep the model simple, viscoelasticity is disregarded in the state equation and the relationship is derived from the linear theory of elasticity. Here, $k_1=2.00 \times 10^7 \text{ g/(s}^2\text{cm)}$, $k_2=-22.53 \text{ cm}^{-1}$, and $k_3=8.65 \times 10^5 \text{ g/(s}^2\text{cm)}$ are all taken constant.



Fig. 2 A systematic arterial tree with compliant vessels

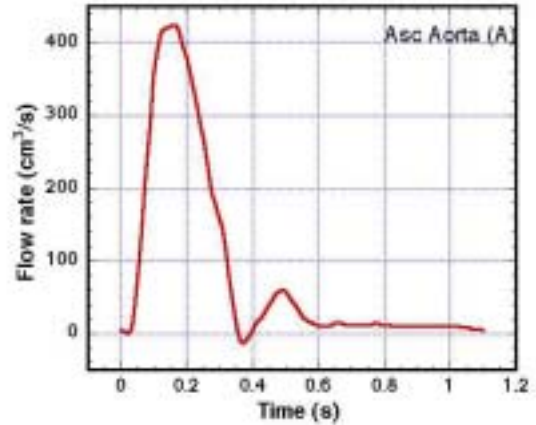


Fig. 3 MR measured flow at Asc. Aorta

A MUSCL-type 3rd-order upwind scheme

With consideration of the consistency with the solutions to the full Navier-Stokes equations, the preceding governing equations are reformed in a vector form \mathbf{U} , and solved in an implicit Euler scheme with a MUSCL-type 3rd-order upwind scheme for the convective terms. A delta form for the increment $\delta \mathbf{U}$ is gained as,

$$\frac{\partial \mathbf{U}}{\partial t} + \frac{\partial \mathbf{F}}{\partial x} = \mathbf{S}, \tag{4}$$

where

$$\mathbf{U} = \begin{bmatrix} A \\ q \end{bmatrix}, \mathbf{F} = \begin{bmatrix} q \\ \frac{q^2}{A} + B \end{bmatrix}, \mathbf{S} = \begin{bmatrix} 0 \\ -\frac{2\pi v q R}{\delta A} + C \end{bmatrix},$$

which is a linear system of equations and can be solved by a tri-diagonal matrix solver efficiently.

Bifurcation conditions are quite important because bifurcations represent an outflow boundary for the parent vessel and an inflow boundary for the daughter vessels. We assume that all bifurcations occur at a point and that there is no leakage so that the continuity in flow volume and the pressure leads to following conditions,

$$q_{pa} = q_{d_1} + q_{d_2}, p_{pa} = p_{d_1} = p_{d_2}, \quad (5)$$

where subscripts pa, d₁, and d₂ represent the parent vessel, and the two daughter vessels, respectively. At the aortic arch, the loss of energy that is expressed in terms of a loss coefficient K is introduced at the inlet of one daughter vessel with a value of K=0.75. At inlet to the arterial tree, i.e., the ascending aorta a magnetic resonance measurement of the flow is imposed as shown in Fig. 3. At outlets, a lumped parameter model by Stergiopoulos et al. is employed, which is a modified windkessel model accounting for both the resistive and the compliant effects of vessels beyond the point of termination. The resulting outflow boundary condition takes the form

$$\frac{dq}{dt} = \frac{1}{R_1} \frac{dp}{dt} + \frac{p}{R_1 R_2 C_T} - \left(1 + \frac{R_1}{R_2}\right) \frac{q}{R_1 C_T}, \quad (6)$$

where $R_1 + R_2 = R_T$ denotes the total resistance of the termination branch, and C_T is the compliance.

2.2 Three-dimensional modeling of hemodynamics in an image-based, realistic vessel

Image-based modeling of a blood vessel

A PATient-Specific Simulator (PASS) for hemodynamics that we developed (Liu, et al., 2001) has formed a foundation for the simulation-based diagnosis and surgery. The PASS is an integrated system, involving an image-based morphological model, a realistic physiological model, and a multi-block, computational mechanical model. The morphological modeling system can reconstruct an anatomic model for vessels and/or organs based on medical images of MRA, US, and CT X-ray, and generate meshes for computation. The physiological modeling is measurement-based, in which blood velocity and pressure are measured by techniques such as MRA and Doppler US. It offers boundary conditions needed by the detailed simulation through a quasi-static hydraulic model.

We here present a computational modeling of aortic hemodynamics. An image-based, realistic anatomic geometry of the aortic arch with bifurcations and taper as well as vessel dynamics is constructed based on the X-ray CT images. The magnetic resonance measurement of inflow waveform at the Asc. aorta is utilized and the profiles of outflow at the Dsc. aorta, the Anonyma artery, the L. Carotid artery, and the L. Subclavian artery are all defined based on the prediction of the one-dimensional model. At inlet to the arterial tree, i.e., the Asc. aorta, the flow profile is directly imposed at the boundary with a uniform flow over the cross-section; but at each outlet three-dimensional velocity profiles are determined on a basis of the predicted flow profiles in a manner of Womersley solution and are imposed at the end of a virtual outlet region connecting to the real outlet boundary.

An FVM-based NS solver

The basic solver is an in-house NS solver in which the incompressible, unsteady Navier-Stokes equations are discretized in a manner of finite volume method (FVM) and are solved in a time-marching manner using the pseudo-compressibility technique by adding a pseudo time derivative of pressure to the continuity equation. Since computational modeling of blood flow requires solving, in the general case, the three-dimensional transient-flow equations in deforming blood vessels the arbitrary-Lagrangian-Eulerian (ALE) description of media is employed, in which the fluid and wall domains are allowed to move to follow the distensible vessels and deforming fluid sub-domain. Here the fluid is assumed to be homogeneous, incompressible and Newtonian. The governing equations are the incompressible, unsteady Navier-Stokes equations, written in strong conservative form for momentum and mass and nondimensionalized in an integral form such that:

$$\int_{V(t)} \text{St} \left(\frac{\partial \mathbf{q}}{\partial \tau} \right) dV + \text{St} \frac{\partial}{\partial t} \int_{V(t)} \mathbf{Q} dV + \int_{S(t)} \mathbf{f} \cdot \mathbf{n} dS = 0, \quad (7)$$

where the last term $\mathbf{f} = (\mathbf{F} + \mathbf{F}_v, \mathbf{G} + \mathbf{G}_v, \mathbf{H} + \mathbf{H}_v)$ expresses the net flux across the cell surfaces. Other terms are defined as:

$$\mathbf{Q} = \begin{bmatrix} u \\ v \\ w \\ 0 \end{bmatrix}, \quad \mathbf{q} = \begin{bmatrix} u \\ v \\ w \\ p \end{bmatrix}, \quad \mathbf{F} = \begin{bmatrix} u^2 + p \\ uv \\ uw \\ \beta u \end{bmatrix}, \quad \mathbf{G} = \begin{bmatrix} vu \\ v^2 + p \\ vw \\ \beta v \end{bmatrix}, \quad \mathbf{H} = \begin{bmatrix} wu \\ wv \\ w^2 + p \\ \beta w \end{bmatrix}, \quad (8)$$

$$\mathbf{F}_v = -\frac{1}{\text{Re}} \begin{bmatrix} 2u_x \\ u_y + v_x \\ u_z + w_x \\ 0 \end{bmatrix}, \quad \mathbf{G}_v = -\frac{1}{\text{Re}} \begin{bmatrix} v_x + u_y \\ 2v_y \\ v_z + w_y \\ 0 \end{bmatrix}, \quad \mathbf{H}_v = -\frac{1}{\text{Re}} \begin{bmatrix} w_x + u_z \\ w_y + v_z \\ 2w_z \\ 0 \end{bmatrix}.$$

In the preceding equations, p is pressure; u , v , and w are velocity components in Cartesian coordinate system, x , y , and z ; t denotes physical time; τ is pseudo time; $V(t)$ is the volume of a cell; $S(t)$ is the surface of the cell; $\mathbf{n} = (n_x, n_y, n_z)$ are components of the unit outward normal vector corresponding to all the faces of a polyhedron cell. Re is Reynolds number and St is Strouhal number. Note that, in the fourth component of Eq. (8), the method of pseudo-compressibility is employed with a time derivative of pressure artificially added to the equation of continuity with a positive parameter β . Note that the term \mathbf{q} associated with the pseudo time is designed for an inner-iteration at each physical time step, and will vanish when the divergence of velocity is driven to zero so as to satisfy the equation of continuity. Details can be found in Liu et al. 2000.

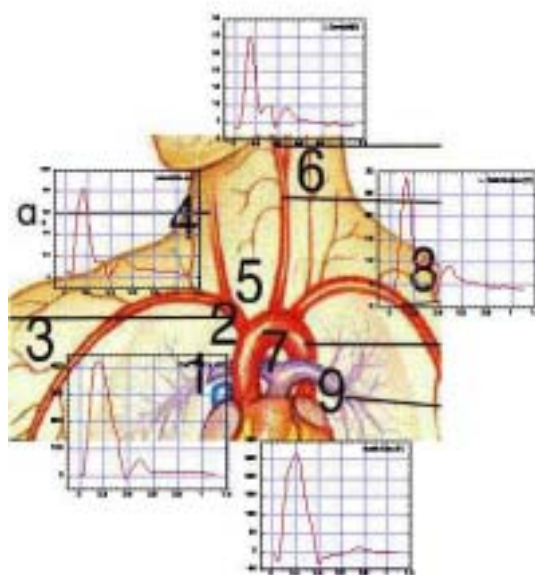
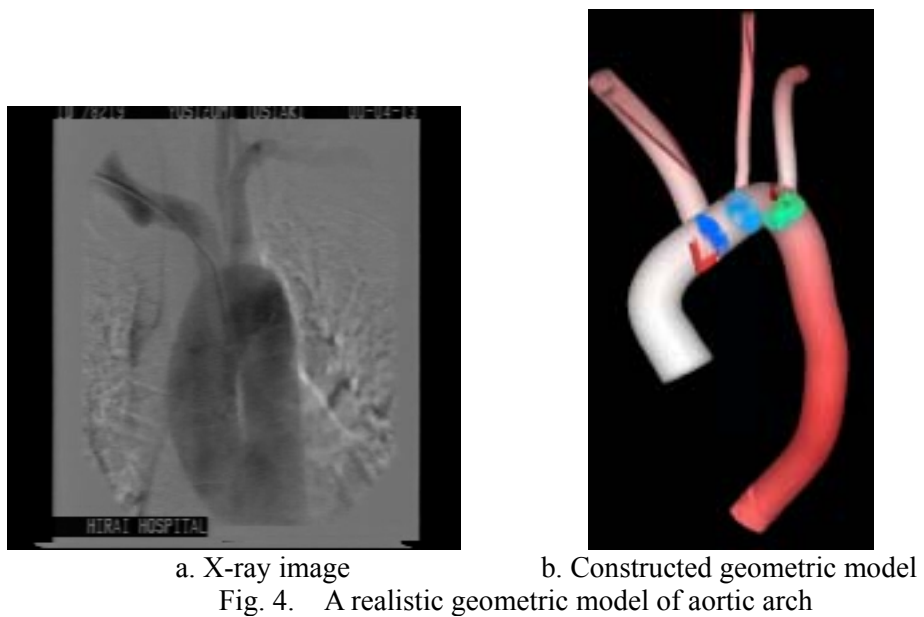
A series of stepwise computations of blood flows in the prototype aortic arch model have been conducted with specific focus on the influence of nonplanarity, bifurcations, dynamics, inflow and outflows on the aorta hemodynamics.

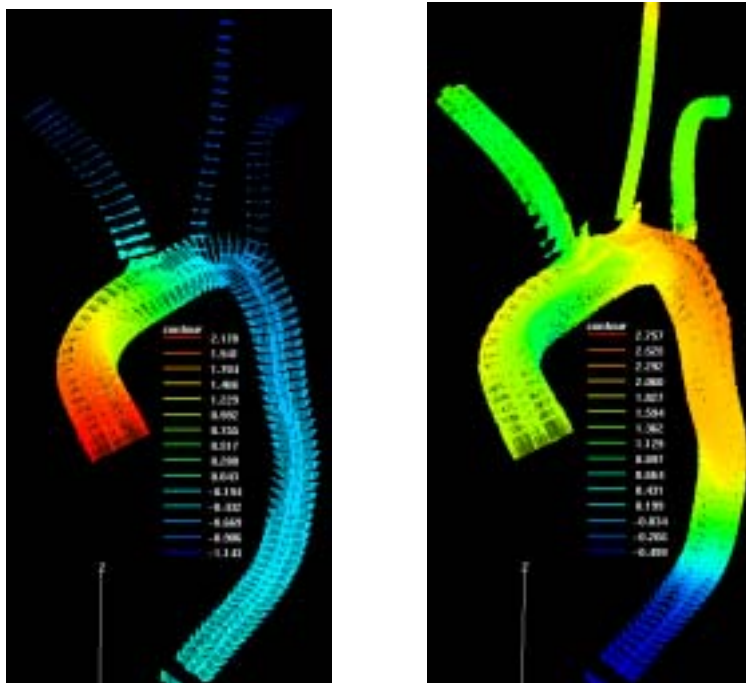
3. Results and discussions

3.1 A prototype multi-scale model of aortic arch

As a prototype multi-scale hemodynamic model we have recently incorporated a recently developed 1D computational model for cardiovascular system into the PASS model. We are aiming at establishing an interactive, multi-scale model in which, not only the global one-dimensional model can provide boundary conditions for the local three-dimensional model in terms of flow rate q and pressure p , but also that the three-dimensional model with realistic geometry can be used to improve the one-dimensional model in terms of feedback of the detailed flow information such as pressure drop.

A prototype multi-scale model of aortic arch as illustrated in Fig. 4 has been constructed; in which an idealized geometric model and a realistic anatomic model based on X-ray images as well as the magnetic resonance measurement of inflow wave at the Asc. aorta are utilized and the profiles of outflow at the Dsc. aorta, the Anonyma artery, the L. Carotid artery, and the L. Subclavian artery are defined based on the prediction of the one-dimensional model (Fig. 5). At inlet to the arterial tree, i.e., the Asc. aorta, the flow profile is directly imposed at the boundary with a uniform flow over the cross-section; but at each outlet three-dimensional velocity profiles are determined on a basis of the predicted flow profiles in a manner of Womersley solution and are imposed at the end of a virtual outlet region connecting to the real outlet boundary.

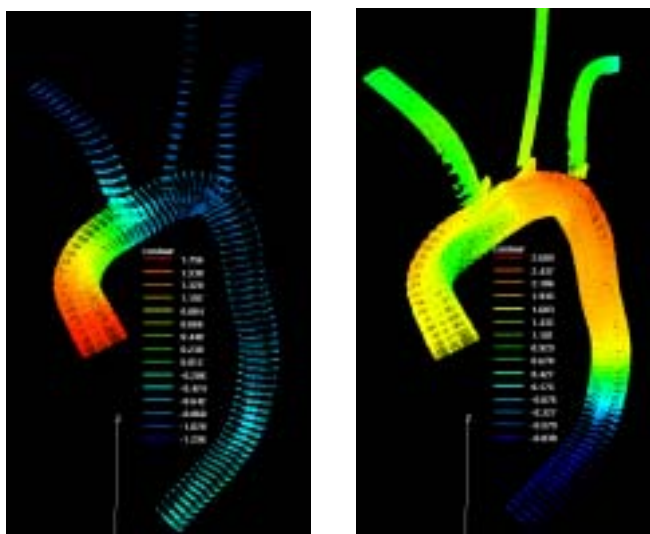




a. Early systole

b. Mid systole

Fig. 6. Velocity vectors and pressure contours in the aortic arch without vessel dynamic influence



a. Early systole

b. Mid systole

Fig. 7. Velocity vectors and pressure contours in the aortic arch with vessel dynamic influence

Given the reference length of the diameter at Asc. aorta, 2.5cm, the top speed based on the maximum flow rate at the Asc. Aorta of approximately 87.6cm/s, the beating period of about 1.1s, the density of 1.055 g.cm³, and the viscosity of 0.049 g/(cm³), we calculated a maximum Reynolds number of 4700 and a Womersley number of 14.0 that corresponds to a Strouhal number of 0.026. The turbulence model is disregarded in this computation and the fluid is assumed to be laminar throughout the complete beating cycle. Fig. 6 and Fig. 7 show the blood flow patterns at a. Early systole and b.

Mid-systole in a form of velocity vectors and pressure contours in the aorta models without (Fig. 6) and with (Fig. 7) vessel dynamic influence, respectively. The color map denotes the pressure increasing from blue to red. Overall, this comprehensive study indicates the following characteristics of blood flow development in the aorta: 1) the non-planarity in geometry can result in the helical flow but only when the core stream flows over the apex of the aortic arch; 2) the bifurcations create strong skewed helical flows in the Anonyma artery, the L. Carotid artery, and the L. Subclavian artery and also lead to complicated separated regions in the aorta in particular at diastole; 3) the vessel dynamics can create and enhance the helical flow in the Asc. aorta (Fig. 6 and Fig. 7) at early-to-mid-systole; 3) the secondary flow at inlet can extend its influence on the blood flow throughout the aorta; and 4) the 1D model-based outflow boundary conditions are physiologically adequate and important which show remarked discrepancy compared with the conventional boundary conditions as zero gradients for pressure and/or velocity at outlet.

Reference

- 1) N. Stergiopoulos, D. F. Young, and T. R. Rogge (1992) Computer simulation of arterial flow with applications to arterial and aortic stenoses, *J. Biomechanics*, **25** (12), pp. 1477-1488.
- 2) P. J. Kilner, et al. (1993) Helical and retrograde secondary flow patterns in the aortic arch studied by three-directional magnetic resonance velocity mapping, *Circulation*, **88** (5), Part 1, 2235-2247.
- 3) L. Zabielski, et al. (1998) Unsteady blood flow in a helically symmetric pipe, *J Fluid Mech* **370**, 321-345.
- 4) H. Liu and T. Yamaguchi (2000) Waveform dependence of pulsatile flow in a stenosed channel, *ASME J. Biomech. Eng.*, **123**, pp. 88-96.
- 5) M. S. Olufsen, C. S. Peskin, W. Y. Kim, E. M. Pedersen, A. Nadim, and J. Larson (2000) Numerical simulation and experimental validation of blood flow in arteries with structured-tree outflow conditions, *Annals of Biomedical Engineering*, **28**, pp. 1281-1299.
- 6) H. Liu, (2001) Global computational modeling of cardiovascular blood flow, *Proceedings of RIKEN Symposium-Computational Biomechanics-*, RIKEN.